

# Al<sub>2</sub>O<sub>3</sub>/TiC/(MoSi<sub>2</sub> + Mo<sub>2</sub>B<sub>5</sub>) Multilayer Composites Prepared by Tape Casting

Guo-Jun Zhang,\*† Xue-Mei Yue† and Tadahiko Watanabe

Department of Inorganic Composite Materials, Kyushu National Industrial Research Institute, Shuku, Tosu, Saga 841-0052, Japan

(Received 3 December 1998; accepted 30 December 1998)

## Abstract

A new multilayer composite (MLC) with a super-plastic layer, a hard layer and a weak interface was proposed in this paper. The hard layer can provide the MLC high temperature strength, the super-plastic layer can deform plastically at high temperatures and disperse the applied stress and stop the advance of the crack, and the weak interface can deflect the propagating crack at room temperature. Such MLC was prepared by tape casting in the Al<sub>2</sub>O<sub>3</sub>/TiC/MoSi<sub>2</sub> + Mo<sub>2</sub>B<sub>5</sub> system in the present work. In this system Al<sub>2</sub>O<sub>3</sub> was as the hard layer, MoSi<sub>2</sub> + Mo<sub>2</sub>B<sub>5</sub> was as the super-plastic layer and TiC was as the weak interface. The microstructures and the stress-displacement behaviors of the MLCs were investigated. It was found that such design is effective on the increase of fracture energy both at room temperature and at high temperatures, and the strength at high temperatures could be remained in a relatively high level. © 1999 Elsevier Science Limited. All rights reserved

**Keywords:** multilayer composites, tape casting, mechanical properties, Al<sub>2</sub>O<sub>3</sub>, silicides.

## 1 Introduction

There are two main problems for structural ceramics: (1) reliability; and (2) cost. Many researchers have been studying these two problems continuously and great progress has been achieved. The low reliability of ceramics comes from the catastrophic fracture behavior under applied stress.

The reason of catastrophic fracture is for lack of energy absorbing mechanisms in the failure process of ceramics. Therefore composite ceramics has been widely studied in the last 20 years. Generally, composite ceramics can be divided into particulate composite, whisker composites; fiber composites and multilayer composites (MLCs). Additionally, some new kinds of composite ceramics have been developed in recent years, such as functionally gradient materials (FGM) and fibrous monolithic ceramics with weak inter-phases.<sup>1</sup> It has been demonstrated that, in contrast to particulate or whisker composites, fiber composites or MLCs with weak interfaces can sustain stresses after onset of fracture. This means that fiber composites and MLCs with weak interfaces are flaw tolerant and reliable for structural applications.

Clegg *et al.*<sup>2</sup> developed a simple way to make tough multilayer SiC with graphite interface layers. The apparent fracture toughness and fracture work of this material increased more than fourfold and a hundredfold respectively. In the last 10 years, the MLCs have been attracting many researchers. One of the popular process used for manufacturing MLCs is tape casting. The studied systems including SiC/graphite, Si<sub>3</sub>N<sub>4</sub>/BN,<sup>3,4</sup> Si<sub>3</sub>N<sub>4</sub> (dense)/Si<sub>3</sub>N<sub>4</sub> (porous),<sup>5</sup> SiC/(glass + fiber),<sup>6</sup> Al<sub>2</sub>O<sub>3</sub>/(Al<sub>2</sub>O<sub>3</sub> + 4 vol% ZrO<sub>2</sub>),<sup>7,8</sup> Al<sub>2</sub>O<sub>3</sub>/fiber-reinforced epoxy composite,<sup>9</sup> MoSi<sub>2</sub>/(MoSi<sub>2</sub> + Al<sub>2</sub>O<sub>3(pl)</sub>),<sup>10</sup> MoSi<sub>2</sub>/SiC<sup>11</sup> and so on. The main feature for the MLCs is that there is a weak interphase between the 'matrix' layers. This weak interphase could be low strength material such as graphite, boron nitride, porous materials, or plastic materials such as fiber reinforced epoxy. In addition, the mechanical properties of a MLC can be controlled by adjusting the bonding strength of the interphase with the 'matrix' layers such in Si<sub>3</sub>N<sub>4</sub>/BN system,<sup>4</sup> in which some Si<sub>3</sub>N<sub>4</sub> was added into BN to adjust the interphase strength. The modeling of the fracture behavior of the MLCs were also investigated in these years.<sup>12,13</sup>

\*To whom correspondence should be addressed.

†Permanent address: Advanced Ceramics Division, China Building Materials Academy, Beijing 100024, People's Republic of China.

In previous work, the authors proposed a novel design to produce high temperature MLCs.<sup>14</sup> The main point of this idea is that a super-plastic material at high temperatures is used as the inter-phase (called super-plastic layer or soft layer) and the 'matrix' (called hard layer) is relatively with good high temperature mechanical properties. This super-plastic layer can act as the dispersing element of applied stress and make the MLC flaw tolerant. Such multilayer structure is something like that of mollusk shell,<sup>15,16</sup> in which the 'hard' phase is  $\text{CaCO}_3$  or  $\text{Ca}_5(\text{PO}_4)_3\text{OH}$ , the 'soft' phase is a proteinaceous substance. The first selected materials system was  $\text{Al}_2\text{O}_3/\text{MoSi}_2$ , in which  $\text{MoSi}_2$  was as the soft layer and  $\text{Al}_2\text{O}_3$  as the hard layer. For improving the high temperature plasticity of  $\text{MoSi}_2$ , 20 wt% of  $\text{Mo}_2\text{B}_5$ <sup>17,18</sup> was added to this layer. However, on the other hand, there is little toughening effect at room temperature because of the strong bonding between  $\text{Al}_2\text{O}_3$  and  $\text{MoSi}_2 + \text{Mo}_2\text{B}_5$  layers. In this work, for improving the room temperature fracture behavior of this MLC, TiC was used as the interphase material for getting a relatively weak interface. Moreover, TiC will become ductile at above  $800^\circ\text{C}$  and also maybe have a good role for the high temperature fracture behavior of this MLC. This paper reports the microstructures and fracture behaviors of  $\text{Al}_2\text{O}_3/\text{TiC}/\text{MoSi}_2 + \text{Mo}_2\text{B}_5$  MLC prepared by hot pressing at different temperatures.

## 2 Experimental Procedure

The raw powders were  $\text{Al}_2\text{O}_3$  (particle size  $0.2\ \mu\text{m}$ ),  $\text{MoSi}_2$  (particle size  $6\ \mu\text{m}$ ) and  $\text{Mo}_2\text{B}_5$  (particle size  $1\ \mu\text{m}$ , Japan New Metal Co. Ltd). The flow chart for the preparation of the MLCs is shown in Fig. 1. The slurry formulation is listed in Table 1. Casting was conducted at  $50\ \text{cm}\ \text{min}^{-1}$  with the doctor blade machine DP-150 manufactured by Sayama Riken Co., Japan. The tape was 160 mm wide and the thickness could be easily adjusted by four measuring gauges. TiC interphase was made by brushing a TiC suspending liquid onto the upper surface of the dried tape. The burning out temperature for organic components in the cast tapes was determined by thermogravimetric analysis

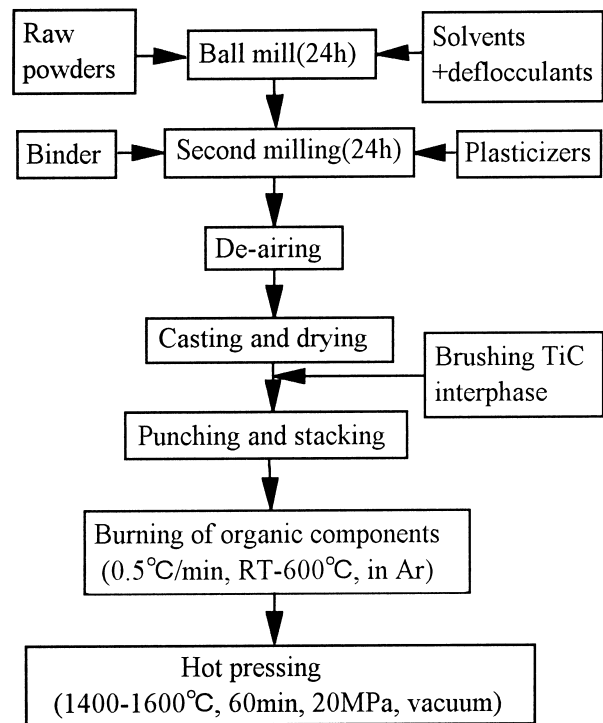


Fig. 1. Flow chart for the preparation of  $\text{Al}_2\text{O}_3/\text{TiC}/\text{MoSi}_2 + \text{Mo}_2\text{B}_5$  MLC.

(TG). The phase compositions of the specimens were analyzed by X-ray diffraction (XRD) method. The hot press temperatures were 1400, 1500 and  $1600^\circ\text{C}$  and the corresponding specimens were marked as MC14, MC15 and MC16, respectively. The bending stress–displacement curves at room temperature were measured by three-point bending method on bars of  $2 \times 4 \times 12\ \text{mm}$  with a span of 10 mm and a crosshead speed of  $0.05\ \text{mm}\ \text{min}^{-1}$ . The bending stress–displacement curves at high temperatures of 1300 and  $1400^\circ\text{C}$  were measured by three-point bending method on bars of  $1.4 \times 3.5 \times 12\ \text{mm}$  with a span of 10 mm and a crosshead speed of  $0.07\ \text{mm}\ \text{min}^{-1}$ . Scanning electronic microscope (SEM) was used to observe the microstructures of the manufactured specimens.

## 3 Results and Discussion

### 3.1 Fractured at room temperature

In all SEM pictures the dark layer is  $\text{Al}_2\text{O}_3$  and the light layer is  $\text{MoSi}_2 + \text{Mo}_2\text{B}_5$ . Figure 2 shows the

Table 1. Slurry formulation for tape casting  $\text{Al}_2\text{O}_3$  and  $\text{MoSi}_2 + \text{Mo}_2\text{B}_5$

Constituent	Function	For $\text{Al}_2\text{O}_3$ (vol%)	For $\text{MoSi}_2 + \text{Mo}_2\text{B}_5$ (vol%)
$\text{Al}_2\text{O}_3$ or $\text{MoSi}_2 + \text{Mo}_2\text{B}_5$	Ceramic powder	21.4	25
MEK	Solvent	38.4	35
2-propanol	Solvent	27.3	25
Dibutyl	Plasticizer	5.6	6.5
Polyvinyl butyral	Binder	6.8	8
Fish oil	Deflocculant	0.5	0.5

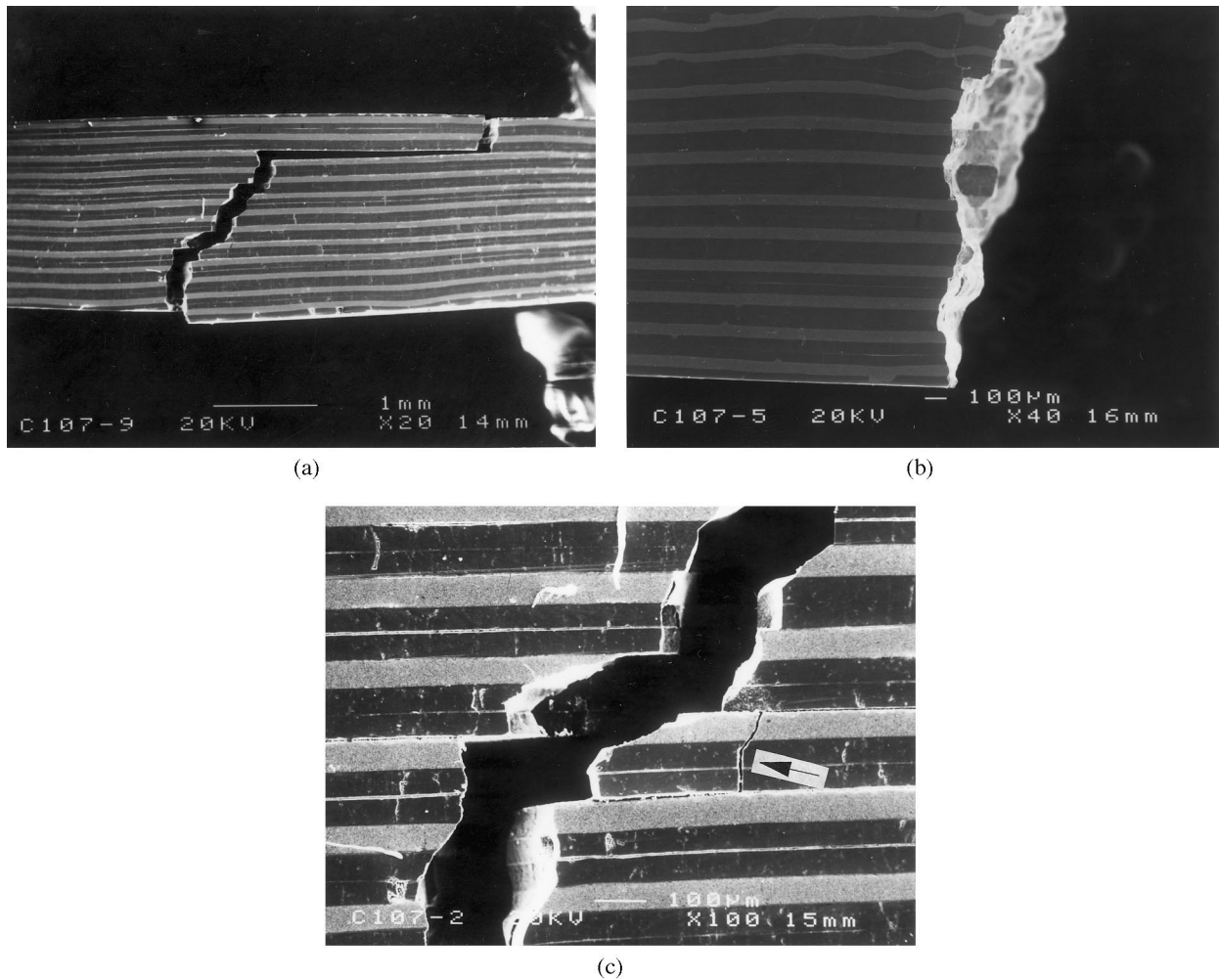


**Fig. 2.** Micrographs of the side surfaces of specimens MC15 and MC16: (a) MC15 specimen; (b) MC16 specimen; (c) higher magnification of MC15 showing the crack deflection.

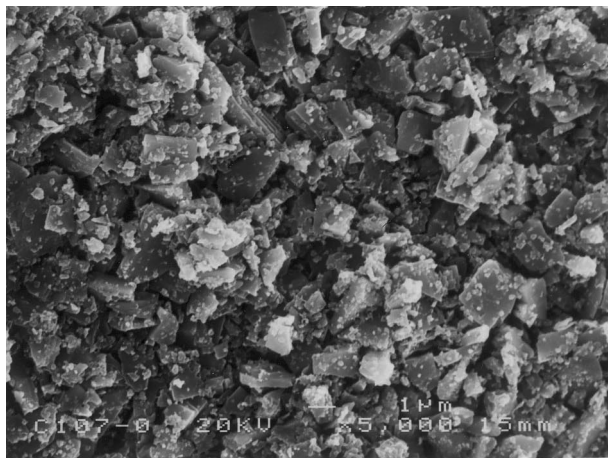


**Fig. 3.** Micrograph of one debris of the specimen MC14.

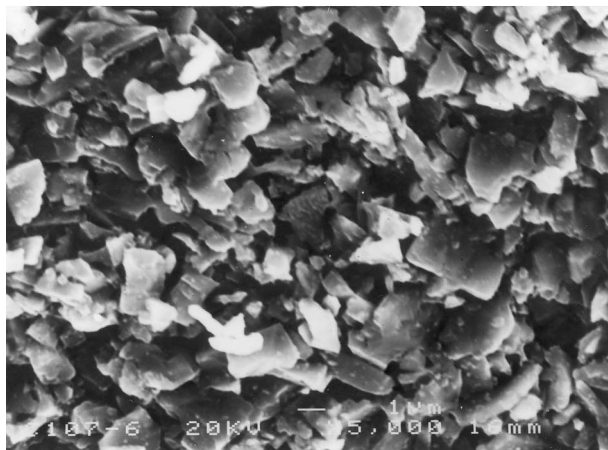
micrographs of the side surfaces of specimens MC15 and MC16. It can be seen that there was large crack deflection in the specimen MC15, but there was small crack deflection for MC16 specimen. In MC15, the crack deflected out of the main stress plane along the weak TiC interface which was vertical to the applied stress. Then the deflected

crack would deflect to the main stress plane after certain propagation along the weak TiC interface. In this process either Al<sub>2</sub>O<sub>3</sub> layer or MoSi<sub>2</sub>+Mo<sub>2</sub>B<sub>5</sub> layer would be broken as shown in Fig. 2(c). For the specimen MC14, the interface bonding strength was too weak to keep the layers together to become a whole block. Figure 3 shows the micrograph of one debris of the specimen MC14.

The microstructures of the TiC interfaces are shown in Fig. 4 for the specimens MC14 and MC15. It can be seen that in the MC14 specimen the sintering of TiC interface looks not to take place, and so resulted in the weak interface in this specimen. For MC15 the sintering of TiC had already taken place, but the bonding strength was still not very high, that is, it was a porous TiC interface with moderate bonding strength. When the hot pressing temperature reached 1600°C, the TiC interface was sintered to a dense layer and resulted in a strong bonding as shown in Fig. 5. Figure 5 shows the side surfaces of MC15 and MC16. In these photos the microstructures of the MoSi<sub>2</sub>+Mo<sub>2</sub>B<sub>5</sub> layers can also be seen. In the MoSi<sub>2</sub>+Mo<sub>2</sub>B<sub>5</sub> layers, the white range is MoSi<sub>2</sub>



(a)



(b)

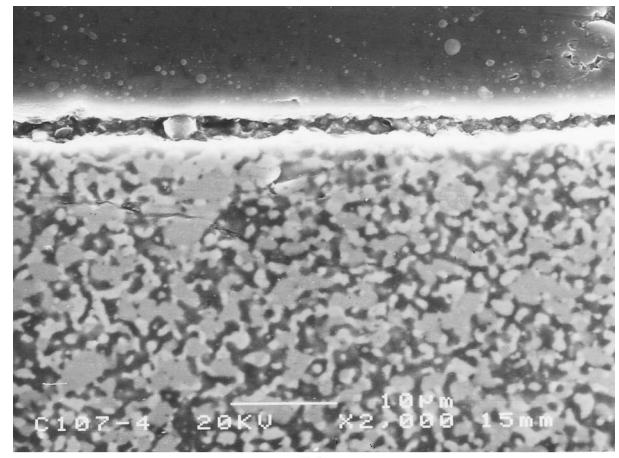
**Fig. 4.** Microstructures of the TiC interfaces of the specimens MC14 and MC15 (a) MC14 specimen; (b) MC15 specimen.

and the gray range is  $\text{Mo}_2\text{B}_5$ . The grain size of  $\text{MoSi}_2$  and  $\text{Mo}_2\text{B}_5$  became coarse with the hot pressing temperature increasing from 1500 to 1600°C, but either was less than 2 μm. On the other hand, the grain size of  $\text{Al}_2\text{O}_3$  was 2~3 μm for MC16.<sup>14</sup>

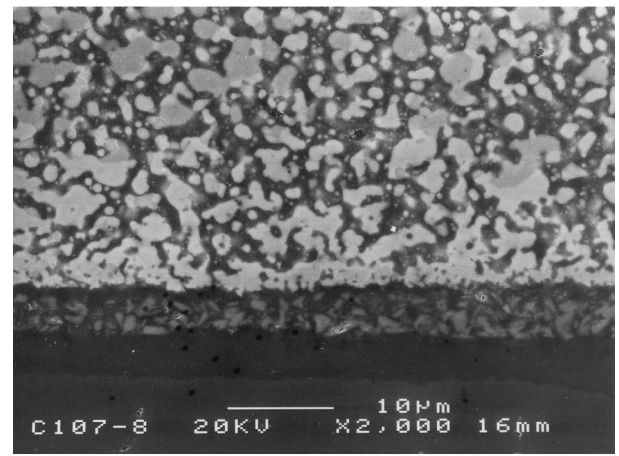
Figure 6 shows the bending stress–displacement curves of MC15 and MC16 specimens fractured at room temperature. For MC15 the large crack deflection showed in Fig. 2(a) was reflected in this curve. However for MC16, because of the strong bonding interface and almost no crack deflection, the bending stress–displacement curve is nearly a linear line.

### 3.2 Fractured at high temperatures

The side surface of MC15 fractured at 1300°C is shown in Fig. 7. This photo shows that the weak TiC interface still play the role in crack deflection at 1300°C. Furthermore, when higher magnification was used to observe the tensile part (the upper surface in Fig. 7) of the side surface of the fractured specimen, many cracks which were vertical to the layers could be found in the  $\text{Al}_2\text{O}_3$  layers as shown in Fig. 8. In  $\text{MoSi}_2 + \text{Mo}_2\text{B}_5$  layers there was not such a crack. This phenomenon was abso-



(a)



(b)

**Fig. 5.** The side surfaces of MC15 and MC16 specimens showing the microstructures of the TiC interfaces (a) MC15; (b) MC16.

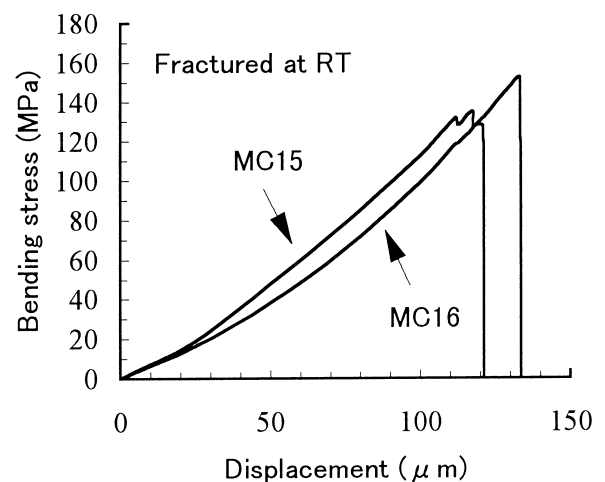


**Fig. 6.** Bending stress–displacement curves of MC15 and MC16 specimens fractured at room temperature.

lutely different from that which appeared in specimen fractured at room temperature as shown in Fig. 2(c). It was considered that at 1300°C the  $\text{MoSi}_2 + \text{Mo}_2\text{B}_5$  layers have already become superplastic. Before the main crack propagating through certain  $\text{Al}_2\text{O}_3$  layer, the  $\text{MoSi}_2 + \text{Mo}_2\text{B}_5$  layers near

this Al<sub>2</sub>O<sub>3</sub> layer would slide and disperse the applied stress in this Al<sub>2</sub>O<sub>3</sub> layer. When the applied stress reached to some limit, many new cracks in this Al<sub>2</sub>O<sub>3</sub> layer would occur. The propagation of these cracks would be stopped by the near MoSi<sub>2</sub>+Mo<sub>2</sub>B<sub>5</sub> layer as shown in Fig. 8(b) and (c) because of that the super-plastic MoSi<sub>2</sub>+Mo<sub>2</sub>B<sub>5</sub>

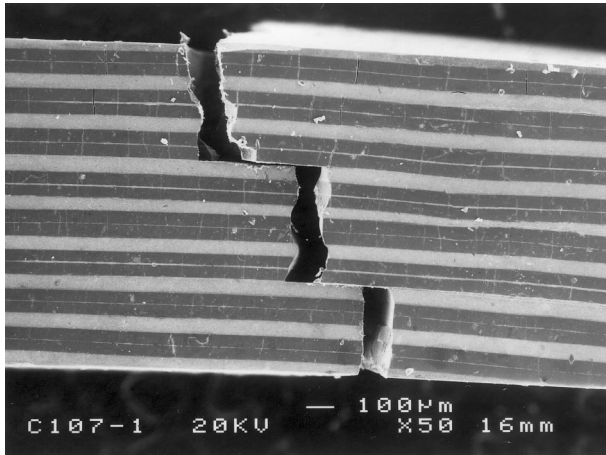


Fig. 7. Side surface of MC15 fractured at 1300°C.

layer could deform plastically and absorb the crack propagating energy or 'absorb' the crack itself as shown in Fig. 8(d).

Figure 9 is the bending stress–displacement curves of MC15 fractured at 1300 and 1400°C. It can be seen that the fracture energy increased

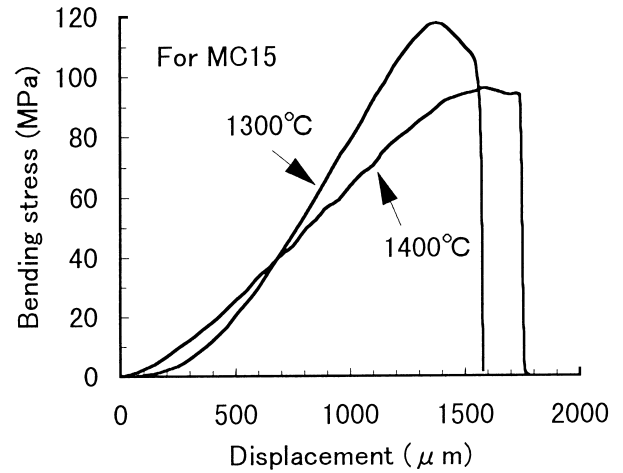
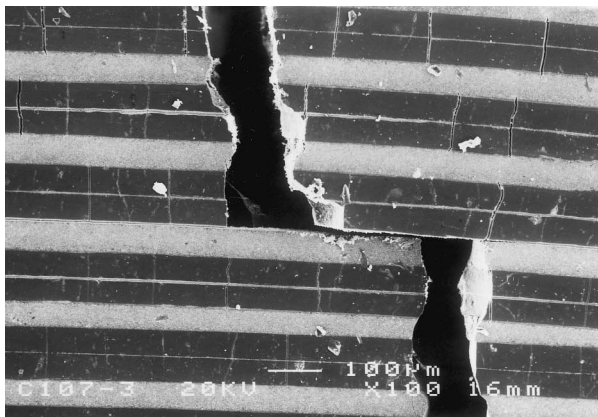
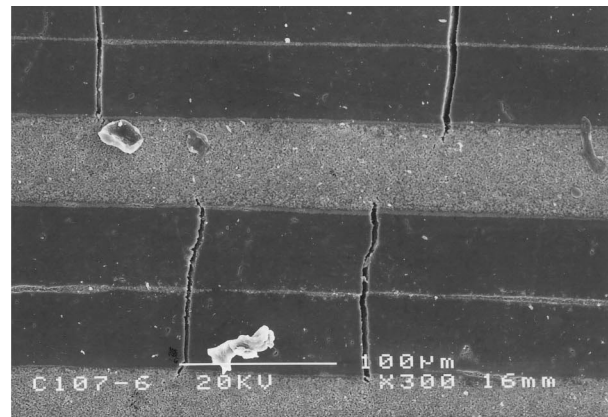


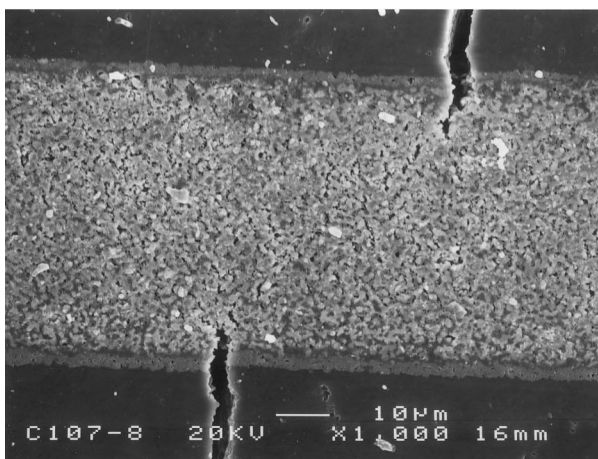
Fig. 9. Bending stress–displacement curves of MC15 fractured at 1300 and 1400°C.



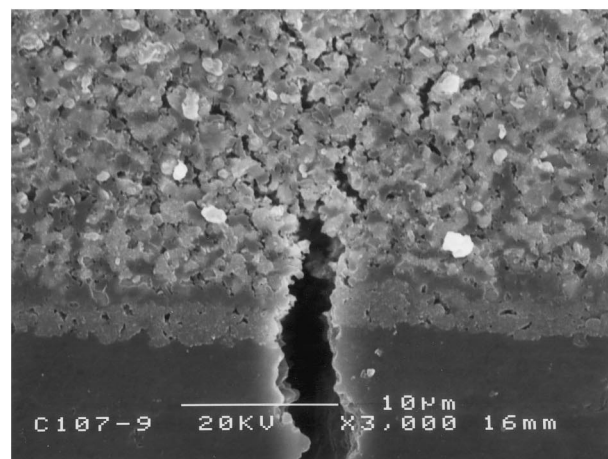
(a)



(b)



(c)



(d)

Fig. 8. Microstructures of cracks in Al<sub>2</sub>O<sub>3</sub> layers fractured at 1300°C: (a) low magnification showing many cracks in Al<sub>2</sub>O<sub>3</sub> layers; (b) higher magnification showing the distribution structure of the cracks; (c) higher magnification showing 'crack connecting' by super-plastic MoSi<sub>2</sub>+Mo<sub>2</sub>B<sub>5</sub> layer; (d) higher magnification showing 'absorbing' of crack by super-plastic MoSi<sub>2</sub>+Mo<sub>2</sub>B<sub>5</sub> layer.

obviously (about 10 times of the value at room temperature according to the area under the bending stress–displacement curves) as well as that most of the strength of the material could maintain at these temperatures.

#### 4 Summary

A new multilayer composite (MLC) of  $\text{Al}_2\text{O}_3/\text{TiC}/\text{MoSi}_2 + \text{Mo}_2\text{B}_5$  with a super-plastic layer ( $\text{MoSi}_2 + \text{Mo}_2\text{B}_5$ ), a hard layer ( $\text{Al}_2\text{O}_3$ ) and a weak TiC interface was proposed in this work. The super-plastic layer can deform plastically at high temperature and disperse the applied stress, and then stop the crack growth. The weak TiC interface can deflect the propagating crack at room temperature. This kind of  $\text{Al}_2\text{O}_3/\text{TiC}/\text{MoSi}_2 + \text{Mo}_2\text{B}_5$  MLC were prepared by tape casting. The microstructures and the stress–displacement behaviors of this MLC were investigated. It was found that such design for multilayer composites was effective on the increase of fracture energy both at room temperature and at high temperatures. Further work is needed on the selection of the material systems of the super-plastic layer, the hard layer and the weak interface. The microstructure design including the optimization of the thickness of each layer and the bonding strength control of the weak interface is also needed to investigate deeply.

#### Acknowledgements

This study was supported by the STA Fellowship program of Japan International Science and Technology Exchange Center (JISTEC) of Science and Technology Agency of Japan.

#### References

1. Kovar, D., King, B. H., Trice, R. W. and Halloran, J. W., Fibrous monolithic ceramics. *J. Am. Ceram. Soc.*, 1997, **80**(10), 2471–2487.
2. Clegg, W. J., Kendall, K., Alford, N.McN., Button, T. W. and Birchall, J. D., A simple way to make tough ceramics. *Nature*, 1990, **347**, 455–457.
3. Liu, H. and Hsu, S., Fracture behavior of multilayer silicon nitride/boron nitride ceramics. *J. Am. Ceram. Soc.*, 1996, **79**(9), 2452–2457.
4. Kovar, D., Thouless, M. D. and Halloran, J. W., Crack deflection and propagation in layered silicon nitride/boron nitride ceramics. *J. Am. Ceram. Soc.*, 1996, **81**(4), 1004–1012.
5. Shigegaki, Y., Brito, M. E., Hirao, K., Toriyama, M. and Kanzaki, S., Processing of a novel multilayered silicon nitride. *J. Am. Ceram. Soc.*, 1996, **79**(8), 2197–2200.
6. Cutler, W. A., Zok, F. W. and Lange, F. F., Mechanical behavior of several hybrid ceramic-matrix-composite laminates. *J. Am. Ceram. Soc.*, 1996, **79**(7), 1825–1833.
7. Boch, P., Chartier, T. and Huttepain, M., Tape casting of  $\text{Al}_2\text{O}_3/\text{ZrO}_2$  laminated composites. *J. Am. Ceram. Soc.*, 1989, **69**(8), C–191–C–192.
8. Requena, J., Moreno, R. and Moya, J. S., Alumina and alumina/zirconia multilayer composites obtained by slip casting. *J. Am. Ceram. Soc.*, 1989, **72**(8), 1511–1513.
9. Folsom, C. A., Zok, F. W., Lange, F. F. and Marshall, D. B., Mechanical behavior of a laminar ceramic/fiber-reinforced epoxy composite. *J. Am. Ceram. Soc.*, 1996, **75**(11), 2969–2975.
10. Tuffe, S. and Wilkinson, S.,  $\text{MoSi}_2$ -based sandwich composite made by tape casting. *J. Am. Ceram. Soc.*, 1995, **78**(11), 2967–2972.
11. Hirvonen, J.-P., Torri, P., Lappalainen, R., Lokonen, J., Kung, H., Jervis, J. R. and Nastasi, M., Oxidation of  $\text{MoSi}_2/\text{SiC}$  nanolayered composite. *J. Mater. Res.*, 1998, **13**(4), 965–973.
12. Phillipps, A. J., Clegg, W. J. and Clyne, T. W., Fracture behavior of ceramic laminates in bending—I. Modelling of crack propagation. *Acta Metall. Mater.*, 1993, **41**(3), 805–817.
13. Folsom, C. A., Zok, F. W. and Lange, F. F., Flexural properties of brittle multilayer materials: I. Modeling. *J. Am. Ceram. Soc.*, 1994, **77**(3), 689–696.
14. Zhang, G. J., Yue, X. M. and Watanabe, T.  $\text{Al}_2\text{O}_3/\text{MoSi}_2$  multilayer composites prepared by tape casting. The First China International Conference on High-Performance Ceramics, Beijing, China, 1 October–3 November 1998, in press.
15. Laraia, V. J. and Heuer, A. H., Novel composite microstructure and mechanical behavior of mollusk shell. *J. Am. Ceram. Soc.*, 1989, **72**(11), 2177–2179.
16. Nicholson, P. S., Nature's ceramic laminates as models for strong, tough ceramics. *Canadian Ceramics Quarterly*, 1995, **2**, 24–30.
17. Watanabe, T. and Shobu, K., The development of plastic  $\text{MoSi}_2$ -boride ceramics. *MRS Int'l. Mtg. on Adv. Mats.*, 1989, **7**, 303–312.
18. Shobu, K., Watanabe, T. and Tsuji, K., Effects of  $\text{Mo}_2\text{B}_5$  addition to  $\text{MoSi}_2$  ceramics. *J. Ceram. Soc. Jpn.*, 1989, **97**(10), 1311–1314.